Temperature dependent friction and wear of magnetron sputtered coating TiAlN/VN

LUO, Quanshun <http://orcid.org/0000-0003-4102-2129>

Temperature dependent friction and wear of magnetron sputtered coating TiAlN/VN

Q. Luo*

Materials and Engineering Research Institute, Sheffield Hallam University, Howard Street, Sheffield, S1 1WB, UK

Abstract

In this paper, a magnetron sputtered nano-structured multilayer coating TiAlN/VN, grown on hardened tool steel substrate, has been investigated in un-lubricated ball-on-disk sliding tests against an alumina counterface, to study the friction and wear behaviours at a broad range of testing temperatures from 25 to 700 ^{0}C, followed by comprehensive analysis of the worn samples using FEG-SEM, cross-sectional TEM, EDX, as well as micro/nano indentations. The experiment results indicated significant temperature-dependent friction and wear properties of the coating investigated. Below 100 ^{0}C, the coating showed low friction coefficient at $\mu \leq 0.6$ and low wear rate in the scale of 10^{-17} $m^3N^{-1}m^{-1}$ dominated by mild oxidation wear. From 100 to 200 ^{0}C, a progressive transition to higher friction coefficient occurred. After that, the coating exhibited high friction of $\mu = 0.9$ at temperatures between 200 and 400 ^{0}C, and simultaneously higher wear rates of ($10^{-16} \sim 10^{-15}$) $m^3N^{-1}m^{-1}$. The associated wear mechanism changed to severe wear dominated by cracking and spalling. From 500 ^{0}C and so on, accelerated oxidation of the TiAlN/VN became the controlling process. This led first to the massive generation of oxide debris and maximum friction of $\mu = 1.1$ at 500 ^{0}C, and then to fast deterioration of the coating despite the lowest friction coefficient of $\mu < 0.3$ at 700 ^{0}C.

Keywords: Magnetron Sputtered Coating; TiAlN/VN; Friction; Wear; High Temperature Tribo-Tests

1. Introduction

Wear resistant hard coatings are highly demanded in modern manufacturing industry to ensure good performance of cutting tools. An important issue has been the understanding of their tribological performance in the increasingly severe working conditions, such as the high working temperatures. TiAlN/VN is a multicomponent nitride coating grown by combined cathodic arc etching and reactive magnetron sputter deposition [1]. TiAlN/VN coated cutting tools have shown excellent wear resistance in machining sticky metals such as aluminium alloys and austenite stainless steel [2-3]. Up to date, comprehensive experimental research has been conducted to study the deposition, structure, mechanical properties, thermal resistance, oxidation kinetics, and tribological properties of the

*Corresponding author. Tel.: +44 1142253649; fax: +44 1142253501.
E-mail address: q.luo@shu.ac.uk (Quanshun Luo)

TiAlN/VN coating [3-8]. Concerning the tribological properties, however, previous experiments were mainly concentrated on the friction and wear properties in room temperature (RT) ambient conditions. For example, the coatings exhibited low friction coefficient at $\mu = 0.4 – 0.6$ and extremely low wear coefficient in a scale of 10^{-17} ~ 10^{-16} $m^3N^{-1}m^{-1}$ in ball-on-disk sliding tests against an alumina ball, which are significantly better than TiN and other TiAlN based coatings [1-4, 7-8]. In the associated wear mechanism studies, Raman spectroscopy of the wear debris detected V_2O_5-type structure [8]. Then more comprehensive analyses of the worn surfaces indicated the formation of an amorphous and multicomponent tribofilm on the worn surface as a result of a dynamic process of wear particle generation, powdering, tribo-oxidation, self agglomeration and adhesion to the parent worn surface [9-11]. The tribofilm was found to be eventually a governing factor of the friction property, and thereafter showed remarkable influence on the prevention of mechanical wear.

It is well known that friction and wear are not intrinsic properties of materials. Instead, they are response of sliding surfaces under the applied test conditions. According to published experimental studies [12-21], environment temperature has significant influence on the sliding friction and wear behaviour of transition metal nitrides. For example, a Cl-containing TiN coating grown by chemical vapour deposition showed extraordinarily low friction of $\mu < 0.2$ and high friction of $\mu = 0.6$ - 0.8 at 100 - 300 ^{0}C [17]. A magnetron sputtered VN coating showed variation of friction coefficient in ball-on-disk tribo-tests against an alumina ball when the testing temperature was increased from room temperature to 700 ^{0}C, in which the maximum coefficients of $\mu = 0.5$ were measured at 300 ^{0}C [19]. For TiAlN/VN coatings, high temperature tribo-tests have been undertaken on limited temperatures, e.g. 500 ^{0}C and 700 ^{0}C in [18] and 300 ^{0}C and 630 ^{0}C in [21]. Surprisingly high friction coefficients of μ = ~0.95 were reported at 300 ^{0}C and 500 ^{0}C. Especially, comprehensive worn surface analyses have updated previous understanding regarding the lubricious effect of V_2O_5 type wear debris.However, while the limited studies indicated remarkable different friction behaviours at different temperatures, it is not still not clear at least in the following aspects: (1) how the friction coefficient of TiAlN/VN changes with varying temperature; (2) the effect of friction coefficient on the wear rate; and (3) relationship between wear, oxidation and friction at elevated temperatures especially when the TiAlN/VN has been found to oxidise at temperatures higher than 550 ^{0}C [27]. For the first aspect, the variation of temperature will bring about changes in the tribo-system, such as the adsorption of oxygen and water molecules on the nitride surface, oxidation of TiAlN/VN at high temperatures, which will certainly influence the friction and wear properties. For the second, high friction was recently found to trigger delamination wear in a TiAlN based TiAlCrYN coating [QL, 2009]. Obviously more experimental work is necessary to understand the dependence of the friction property on the test temperature.

In this paper, the sliding friction and wear behaviours of the TiAlN/VN coating, for a range of testing temperatures from RT to 700 ^{0}C, have been experimentally studied under ball-on-disk test conditions against an alumina counterface. The purpose of the designed tribotests has been to determine the relationship between the friction coefficient and the test temperature. Considering that previous tribological research on the TiAlN/VN coatings had gained understanding of the friction and wear mechanisms at ambient conditions, the content of this paper is focused on the friction property at elevated temperatures, especially on the influence of the high test temperature on the wear mechanism.

2. Experimental

2.1. Coating deposition

The TiAlN/VN coating to be investigated was deposited on pre-hardened (HV7.9 GPa) and polished BM2 tool steel coupons, by the combined cathodic arc vanadium-ion etching and reactive unbalanced magnetron sputtering deposition. In the employed Hauzer Techno HTC 1000-4 Coating unit, two vanadium targets (99.9%) and two TiAl targets (Ti:Al = 50:50 in atomic ratio) were used in the sputtering deposition in a common Ar + N_2 atmosphere at a total pressure of 4.5×10^{-3} mbar at a substrate temperature of 450 ^{0}C. The total coating thickness was 3.2 μm, being determined using the ball crater method.

2.2. Tribo-Tests

Sliding wear tests were undertaken in ambient air using a high-temperature ball-on-disk tribometer (HT tribometer, CSM Instruments SA, Switzerland) against a counterface of an α-Al_2O_3 ceramic ball of 6-mm in diameter. The selected testing temperatures were RT (25 ^{0}C in this case), 70, 100, 120, 150, 200, 300, 400, 500, 600 and 700 ^{0}C. One test was carried out for each temperature except for temperatures of RT, 200, 400, 500 and 700 ^{0}C in which two tests were run. A constant sliding speed of 0.1 m•s^{-1} were applied in the sliding tests. Most of the tests to measure the steady-state friction coefficient were conducted at a relatively low normal load of 1 N and for approximately 15,000 sliding cycles, whereas those to determine the wear coefficients were at a high normal load of 5 N and run much longer, e.g. up to 150,000 cycles in order to create a measurable depth of wear track. In the beginning of each test, the high temperature chamber accommodating the sliding unit was pre-heated at approximately 4 – 5 ^{0}C per minute to reach the pre-programmed test temperature and was stabilized for 15 minutes. During the test, the tangential force applied on the ball sample was continuously acquired to the computer at a preset frequency of 1 Hz to record the variation of friction coefficient versus the sliding distance or the disk rotating cycles.

2.3. Characterization

The as-deposited and tested coatings were analysed using various techniques, including scanning electron microscopy (SEM), transmission electron microscopy (TEM), and mechanical testing. SEM analyses were conducted using a Philips XL-40 and a FEI Nova-200 FEG-SEM, both having attached energy dispersive X-ray (EDX) spectroscopic chemical analysis. TEM observations were carried out on a Philips CM20 STEM and JEOL 2010 FEG-TEM, both operating at 200 KV and the latter offering electron energy loss spectroscopy (EELS) availability. TEM samples were prepared using a Gatan-691 precision ion polishing system (PIPS). Details of TEM sample preparation can be found elsewhere [6, 9-10].

For the mechanical testing, nano-indentation test was conducted employing a CSM Nano-Hardness Tester using a Berkovich indenter at a load of 50 mN, which calculated the plastic hardness value using the integrated Oliver-Pharr model. The hardness value was averaged from 14 measurements. The Knoop hardness was measured using a Mitutoyo Micro-hardness Tester at loads of 25g and 10g respectively, whereas the lengths of the indents

were measured in FEG-SEM images. The residual stress was determined using the XRD-sin$^2\psi$ technique using the diffraction peak of its {220} lattice planes. The adhesion was measured as the critical load of coating spallation in standard scratch test.

3. Results

3.1. Microstructure and mechanical properties

SEM observations show sub-micron scale cellular-like rough surface of the TiAlN/VN coating, Figure 1. Such surface morphology refers to dense columnar grains with sub-dense column boundaries as shown in more details in previous research [6]. The insert in Figure 1 is a low-magnification view of large defect grains protruding on the relatively smooth surface. The defect grains were caused by metal droplets injected during the cathodic arc metal-ion etching [22].

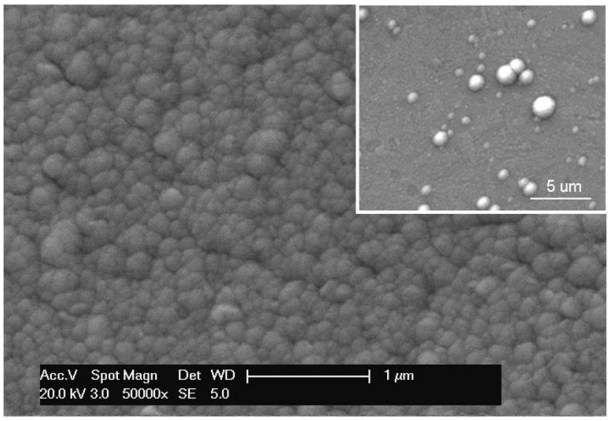

Figure 1 A high resolution SEM image showing sub-micron scale cellular cells of the growth top of the TiAlN/VN coating. The insert is a low-magnification image showing arc-droplet induced growth defect grains (the bright contrast areas).

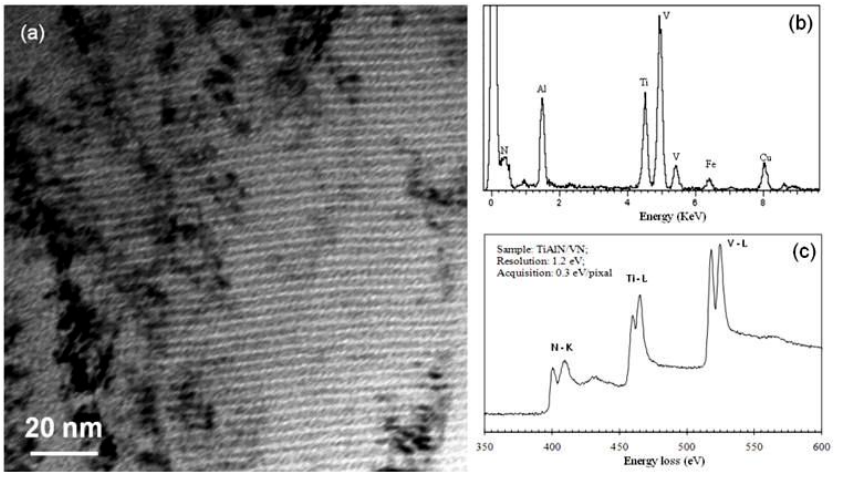

Figure 2 (a) A cross-sectional TEM bright field image showing nano-scale multilayer fringes; (b) An EDX spectrum and (c) an EEL spectrum showing chemical composition of the TiAlN/VN.

Figure 2 shows TEM observation and chemical analyses of the TiAlN/VN coating. In Figure 2a, the coating exhibited arch-like multilayer fringes, being consistent to the surface roughening in Figure 1. The TiAlN and VN bi-layer thickness was measured to be 3.2 nm. Selected area diffraction analysis (not showing here) indicates NaCl-

type cubic crystalline structure with preferred growing orientation (220). The TEM-EDX analysis indicates chemical contents of Al, Ti, V and N, Figure 2b. The TEM-EELS analysis shows, at much higher energy resolution well-defined characteristic edges N-K, Ti-L and V-L, Figure 2c. In particular, the N-K edge consists of two sharp peaks and one broad peak, suggesting the stoichiometric nitrogen concentration [23-25]. Table 1 shows the hardness, residual stress and adhesion properties of the TiAlN/VN coating.

Table 1 Mechanical properties of TiAlN/VN coating

Knoop hardness Load: 25g	Plastic hardness Load: 50 mN	Residual stress	Adhesion
31.7 ± 4.5 GPa	31.4 ± 2.6 GPa	- 5.74 ± 0.88 GPa	46.8 ± 2.1 N

3.2. The temperature dependent friction behaviour

Figure 3 shows a few examples of friction curves obtained at various testing temperatures. Each curve records the friction coefficient variation from running-in to the long-term steady state friction. Whereas the running-in friction was found to be attributed to the initial wear particle generation and the subsequent formation of a tribofilm [26], this study has been more focused on the steady state friction coefficient. For this purpose, the friction coefficient data, being acquired in the steady state period in each test, were processed to calculate the average value and standard deviation.

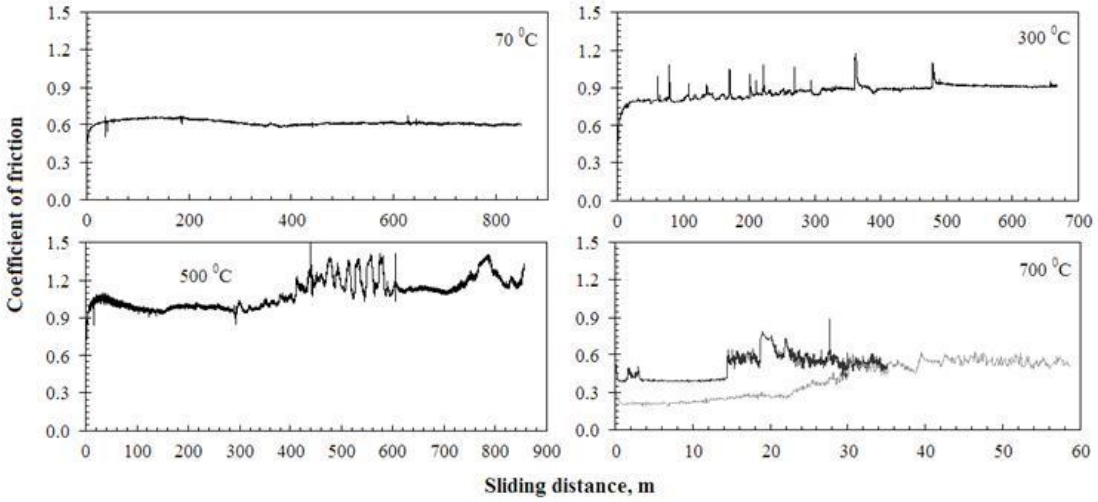

Figure 3 Friction coefficient curves at various testing temperatures.

The overall relationship between the steady state friction coefficient and the test temperature is shown in Figure 4. The friction coefficients measured can be classified into several regions with increasing test temperature. The Regions I and III show relatively temperature independent friction coefficients of μ = 0.60 – 0.61 and μ = 0.86 – 0.89 respectively. The highest and lowest coefficients of friction are μ = 1.1 at 500 ^{0}C (Region IV) and μ = 0.24 at

700 ^{0}C (Region V) respectively. In addition, three temperature ranges are recognised which shows steep variation of friction coefficient, namely between 100 and 200 ^{0}C (Region II), from 400 to 500 ^{0}C, and from 600 to 700 ^{0}C.

It was noticed that, the coating surface became discoloured from 500 to 700 ^{0}C due to oxidation, which was confirmed by subsequent SEM-EDX analysis and is consistent to the iso-thermal oxidation results [6, 18, 27, 28]. As the oxidation may have resulted in the loss of the intrinsic structure and mechanical properties of the nitride coating, the current research focus has been on the samples being tested at temperatures not exceeding 500 ^{0}C.

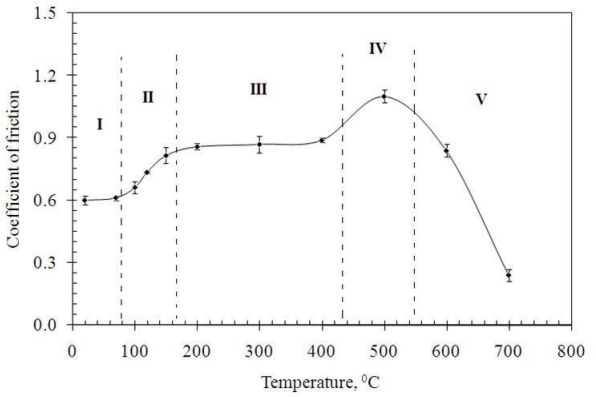

Figure 4 The temperature dependent average friction coefficient of the TiAlN/VN coating in the steady-state sliding period.

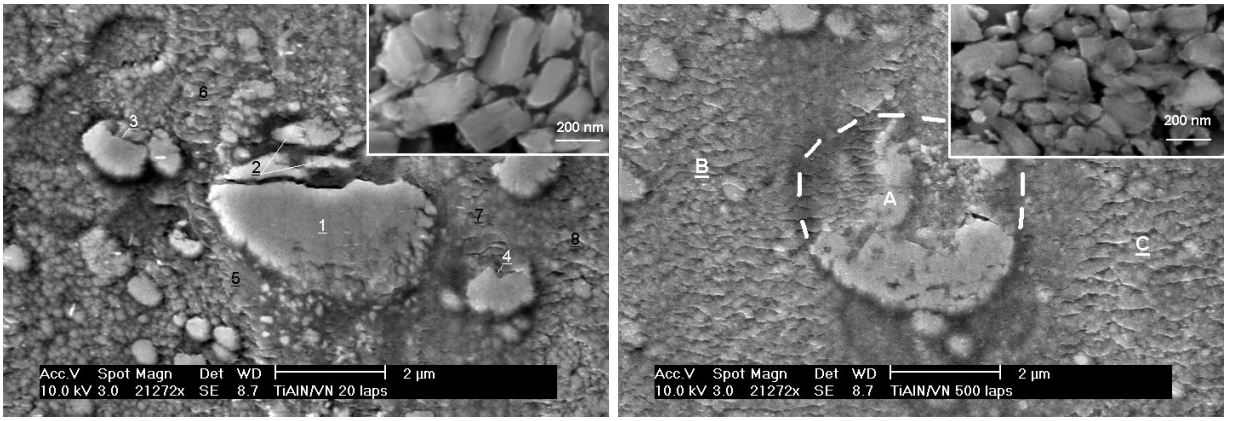

Figure 5 Mechanical wear and tribofilm generation of the TiAlN/VN coating observed after sliding wear at room temperature. (a) After 20 cycles of sliding, a large defect grain in the middle of the imaged area (labelled 1) shows surface flattening and spalling wear (labelled 2). Two smaller sized defect grains also show spalling wear (labelled 3 and 4). The fish-scale-like patterns, labelled 5 - 8, indicate initial form of tribofilm. The insert in the upper-right corner shows initial wear particles extrapped along the wear track edge. (b) A large defect grain (labelled A) observed on the 500-cycle wear track had been mostly worn by spalling. The remaining area (labelled B and C) is full of fish-scale like patterns indicating the developing tribofilm. The insert in the upper-right corner indicates reduced wear particle size after longer period of sliding wear.

3.3. Initial wear and tribofilm formation at room temperature

In the very early stage of a tribotest, initial mechanical wear took place on the droplet-induced growth defect grains in the form of localised fracture. In Figure 5a, the SEM image shows cracking and spalling in such a large defect grain after only 20 cycles of the sliding, whereas the insert illustrates the size of the initial wear particles. The wear particles generated were entrapped subsequently in the sliding contact, causing three-body sliding/rolling abrasive wear of the coating surface and fracturing of the wear particles themselves. The latter led to the formation of a tribofilm adhesively attached on the worn surface. Figure 5b shows the produced fish-scale like tribofilm, as well as further wear of a droplet defect grain, after 500 cycles of sliding.

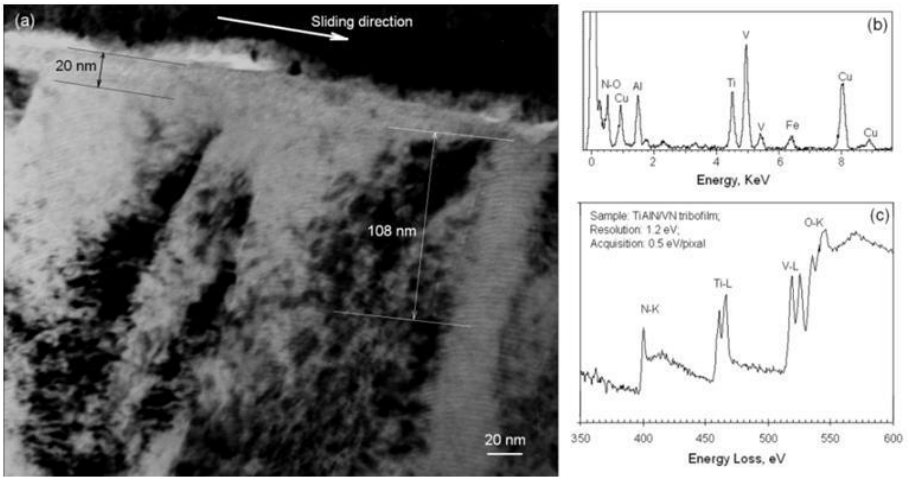

Figure 6 Analytical TEM of the worn TiAlN/VN coating. (a) A longitudinal section of the worn surface show a 20 µm thick tribofilm attached on the top of the worn surface. Beneath that is a depth of approximately 108 nm in which the column grains show slight bending deformation following the sliding direction. (b-c) The EDX and EEL spectra of the tribofilm show its chemical composition of Al, Ti, V, N and O. Note the nearly-edge structure of N-K being different from the N-K edge shown in Figure 2c. The Cu peaks in the EDX spectrum were attributed to TEM sample preparation.

Figure 6 shows the TEM longitudinal cross-sectional imaging and the associated EDX and EELS chemical analyses of a 20 nm thick tribofilm formed on the TiAlN/VN worn surface after approximately 150,000 sliding cycles of sliding wear at room temperature. The content of Al, Ti and V in the tribofilm was almost identical to the parent nitride coating. EELS analysis indicates high intensity O-K and N-K edges, suggesting co-existence of nitrogen and oxygen. Note that the N-K edge has a shape different from the as-deposited TiAlN/VN nitride (Figure 2c), indicating that the nitride debris entrapped in the tribofilm had sub-stoichiometric nitrogen [23-25]. Beneath the worn surface, the TiAlN/VN columns show likely bending deformation towards the sliding direction in a depth of about 100 - 110 nm, although the deformation is not so significant as compared to the deformation of other nitride multilayers in more severe sliding wear [29-30].

3.4. Wear at 200 – 400 ^0C

After 15,000 cycles of sliding tests at 200 - 400 ^{0}C as shown in Figures 1, the coatings showed very small depth of wear. An example is shown in Figure 7. Figure 7a shows 2-dimensional profile of the 400 ^{0}C tested wear track,

in which the depth of wear was almost immeasurable. Part of the worn surface is covered with tribofilm having sub-micron scale thickness. As observed at high magnification, the wear had just polished the rough profile of the coating surface, seeing Figure 7b as compared to Figure 1a.

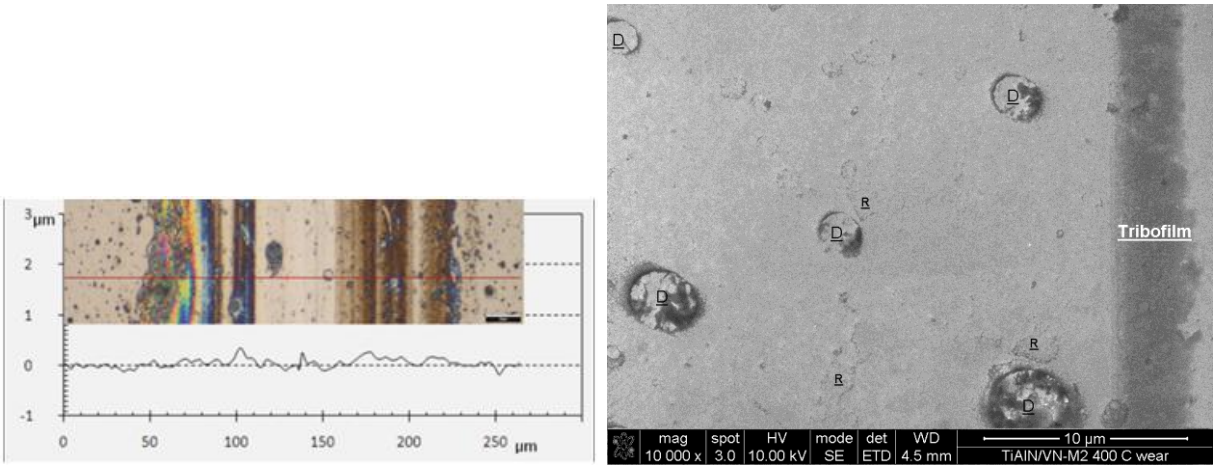

Figure 7 (a) A chart of 2-dimensional profilometric measurement made across the whole width of the TiAlN/VN wear track obtained after 10,000 cycles of sliding wear at 400 ^{0}C. Position of the profilometric scanning in illustrated in the attached optical micrograph. The bright region in the middle indicates smooth worn surface of almost immeasurable depth, whereas the dark contrast bands show attached tribofilms. (b) A FEG-SEM image of the worn surface shows only polishing wear of the rough coating surface (R-labelled regions denoting the remaining rough features of the as-deposited coating), flattened growth defect grains (labelled D) as well as a narrow band of tribofilm.

In the clean and smooth regions of the obtained worn surfaces, Knoop indentations were made, at the minimum load of 10 g, to detect any work hardening caused by plastic deformation, as such deformation was observed after sliding tests under similar circumstances, e.g. in Figure 6a. The results are shown in Figure 8. The RT worn surface shows hardness in a range of 39.5 - 39.9 GPa, being comparable to the as-deposited coating. In contrast, the three worn surfaces tested at elevated temperatures show higher hardness values of 44.0 - 50.0 GPa. In the Knoop indentation, the lengths of the obtained indents were approximately 5.5 µm, which refer to depths of the indentation between 180 - 210 nm. Assuming that the depth of plastic deformation was 100 nm according to Figure 6a, approximately 85% of the indent volume was in the deformed layer. Therefore, despite that the measurements shown in Figure 8 are not the acceptable hardness of the worn surface deformation layer, nevertheless, the deformed layer made significant contribution to the increased hardness. In other words, the Knoop indentation provided a good estimation of the sliding wear induced work hardening.

In order to evaluate the wear coefficient of the coating, long term tribotests were made at 200 and 400 ^{0}C respectively. The results are listed in Table 2. The wear test at 200 ^{0}C ran for a total duration of 146,000 cycles. The first 54,000 cycles exhibited smooth variation of friction coefficient whereas, after that, the friction curve showed substantial fluctuations and higher friction. Such behaviour was caused by the occurrence of cracking and spalling failures of the coating. These have been confirmed by visual inspection, profilometric measurement and SEM

observation after the test. Therefore, the wear test at 400 ^{0}C was terminated sooner seeing the fluctuation of the friction curve. As measured in the smooth areas of the wear tracks, the coating exhibited coefficients of wear of 19.8×10^{-17} and 12.0×10^{-17} $m^3N^{-1}m^{-1}$ at 200 and 400 ^{0}C respectively, which are several times higher than the wear coefficient obtained at room temperature test, Table 2.

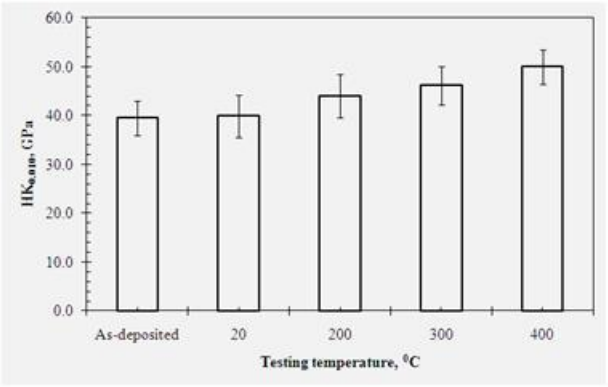

Figure 8 Knoop hardness of the worn surfaces versus the test temperature, measured at an indenting load of 10 g.

Table 2 Results of long term tribotests at elevated temperatures, at applied load 5 N, sliding speed 0.1 $m \cdot s^{-1}$.

	200 ^{0}C	400 ^{0}C	29 ^{0}C
Wear track radius, mm	6.0		
Sliding distance, m	5,506	3135	15,040
Sliding cycles	146,050	68,700	239,263
Coefficient of friction	0.89	0.91	0.58
Depth of wear, μm	1.42 / 13.50*	1.12	-
Coefficient of wear, 10^{-17} $m^3N^{-1}m^{-1}$	19.8 / 766*	12.0	3.48

Note: The second values in the wear depth and coefficient at 200 ^{0}C were measured in the spalling area.

Figure 9 shows SEM observations of the spalling wear and cracking of the 200 and 400 ^{0}C tested worn surfaces respectively. In addition, a longitudinal cross-sectional TEM was also prepared from the 200 ^{0}C tested wear track, to observe the cracking behaviour underneath the worn surface. A typical cross-sectional TEM image is shown in Figure 10. In Figure 9a, the upper-left region is a spalling pit partly filled with wear debris. The TiAlN/VN coating in the adjacent area had developed cracks which would have led to spalling failure if the test were run longer. Figure 10 indicates that substantial crack propagation had been in progress below and parallel to the worn surface. In Figure 9b, the coating surface exhibits parallel cracks distributing along the wear track. The dark contrast substance attached in front of each crack is transferred wear debris of the alumina counterpart, which was confirmed by EDX analysis during the SEM observation.

3.5. Wear at 500 ^{0}C

The wear test at 500 ^{0}C was terminated after 15,120 sliding cycles or a sliding distance of 855 m. The coating surface was found to be remarkably discoloured due to oxidation. Pronounced oxidation of the coating made it impossible to measure the depth of wear using the linear profiling method. The oxidation in the un-tested TiAlN/VN surface was confirmed by SEM observation and the associated EDX analysis. In Figure 11a, the bright short bars were recognised as product of initial oxidation. This phenomenon was comparable to our previous iso-thermal oxidation study of the coating that the onset oxidation of the coating was found to be around 550 ^{0}C [6, 28].

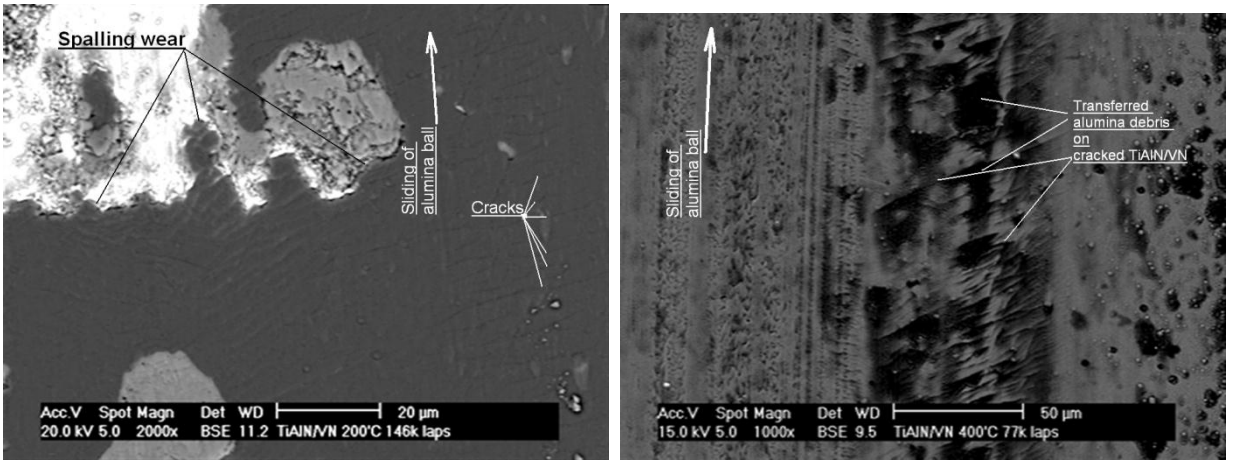

Figure 9 Back scattered electron images of the worn TiAlN/VN surfaces subjected to wear at applied normal load of 5N and sliding speed of 0.1 m·s^{-1} against an alumina ball. (a) After 146,000 sliding cycles at 200 ^{0}C, the worn surface was full of parallel cracks (generating dark BSE contrast) perpendicular to the sliding direction. The upper-left is the exposed steel substrate after adhesive spalling wear of the coating. (b) After 77,000 sliding cycles at 400 ^{0}C, the worn surface exhibited parallel cracks. Along with the cracked edges were wear debris of the alumina counterface (showing dark contrast).

The worn surface was found to be covered with plenty of wear debris, which formed fish-scale-like agglomerates along the wear track, Figure 11b. EDX analysis confirmed the co-existence of oxygen and nitrogen in the wear debris, Figure 11c. Such fish-scale-like features indicate the occurrence of severe shear deformation of the tribofilm during the sliding wear.

The 500 ^{0}C worn sample was also analysed using cross-sectional TEM, as shown in Figure 12. An amorphous tribofilm was found on the top of the worn surface. TEM-EDX analysis suggested its multicomponent oxide chemical composition. The remaining TiAlN/VN nitride still exhibited columnar morphology and nano-scale multilayer fringes. However, some of the TiAlN/VN columns beneath the worn surface showed an arch-like front edge. Beyond the edge the structure became less dense as indicated by the locally brighter imaging contrast. Similar arch-like bright edge have been observed in iso-thermally oxidised TiAlN/VN coating [28], whereas the edge was identified as the interface of the oxidation. Therefore, at least some of the TiAlN/VN grains had experienced static oxidation beneath the worn surface. In other words, static oxidation of the TiAlN/VN nitride might have become a leading process prior to the sliding wear.

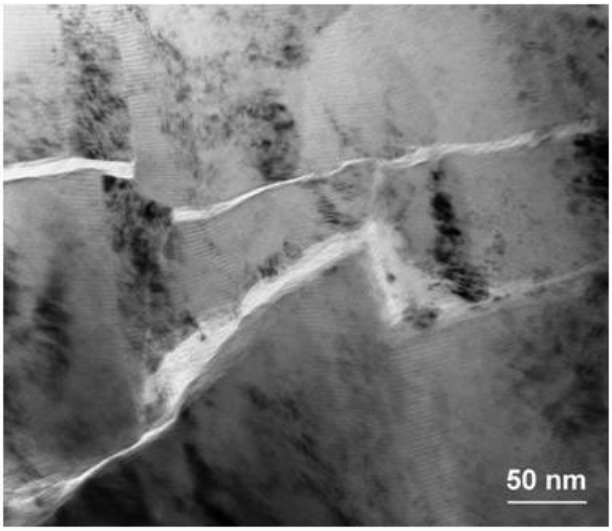

Figure 10 A longitudinal cross-sectional TEM bright field image showing subsurface cracks of the worn TiAlN/VN coating after the 200 ^{0}C test.

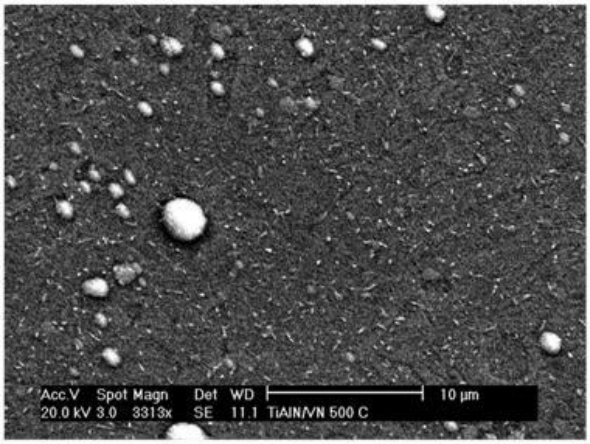

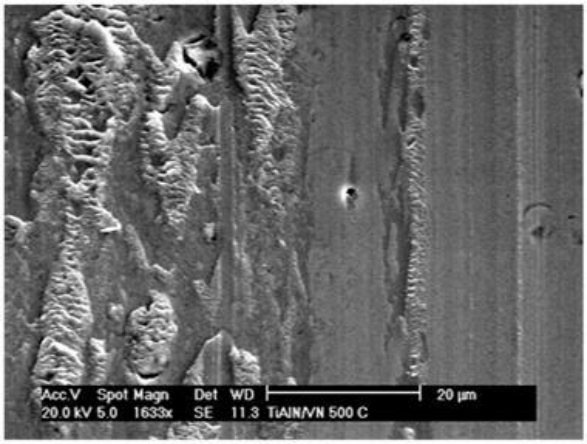

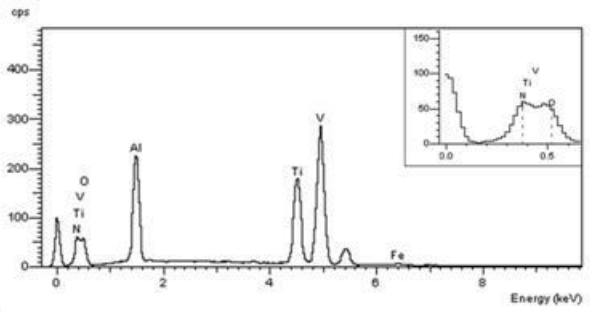

Figure 11 SEM and EDX analysis of the TiAlN/VN coating after the 500 ^{0}C wear test. (a) The un-tested area shows generally the as-deposited surface morphology in addition to the dispersed needle-like fine particles of initial oxidation product. (b) The worn surface shows both smooth area (on the right hand side) and transferred wear debris or thick tribofilm (fish-scale like patterns on the left hand side). (c) An EDX spectrum of the tribofilm shows the coexistence of oxygen and nitrogen, indicative of tribo-oxidation.

4. Discussion

This paper reports that the overall steady friction coefficient of the TiAlN/VN coating / alumina system can be classified into four regions separated by three temperature-dependent transitions, Figure 2. The four regions include low coefficients of 0.6 at temperatures lower than 100 ^{0}C, high coefficients of 0.86 - 0.89 at 200 - 400 ^{0}C, the highest coefficient of 1.1 at 500 ^{0}C, and the lowest coefficient of 0.24 at 700 ^{0}C. The three temperature-dependent transitions refer to the steep variations of friction coefficient in the temperature ranges 100 - 200 ^{0}C, 400 - 500 ^{0}C, and 500 - 700 ^{0}C. The coefficients at RT and 500 - 700 ^{0}C are in good consistent to previous experiment results of similar TiAlN/VN coatings [3-4, 8, 18, 21]. This section will discuss the temperature-dependent mechanisms of friction and wear.

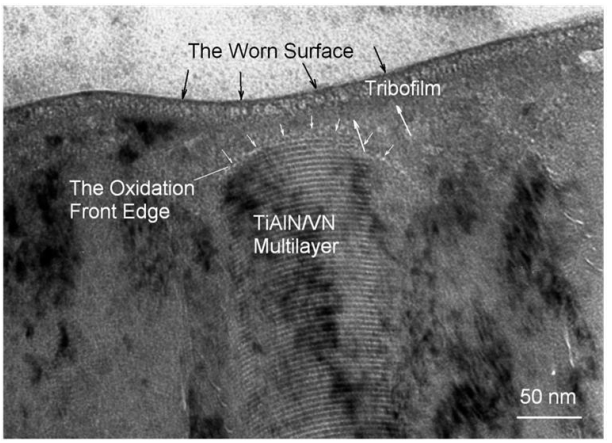

Figure 12 Cross-section TEM bright field images of the 500 ^{0}C worn surface showing oxidation of a columnar TiAlN/VN nitride grain beneath the tribofilm.

4.1 Effect of tribofilm formation on the friction and wear behaviours

In un-lubricated ball-on-disk tribo-tests, a third body plays an important role in determining the friction behaviour, including the entrapped wear debris, tribo-oxidation, and the formation of a tribofilm. In the sliding wear of metals [31], after the generation and agglomeration of wear particles in the initial wear, the severity of sliding friction depends strictly on the adhesive interactions of the wear debris. Therefore the role of a lubricant is related to the breaking or weakening of the interfacial bonding. In the current research, wear debris engagement and tribofilms were involved in all the tribotests, seeing Figures 5, 6, 9 and 11, indicating their significant influence on the friction coefficient. More details of the relationship between tribofilm formation and the running-in friction property can be found in a recent paper published elsewhere [26].

In addition, tribo-oxidation has been found to be a general phenomenon in the tribo-tests regardless the testing temperature. Regarding the mechanism of tribo-oxidation, a two-step model was proposed, in literature [32], i.e. the initial oxidation film at the asperity contact tips and the subsequent breaking of the film after reaching a critical film thickness. The current research found that, tribo-oxidation took place in such a dynamic process which is obviously different from the above model. The initial sliding contact resulted in prompt fracture of the growth defect grains to generate the original wear particles. Then during the running-in period, tribo-oxidation occurred in the progressive

powdering wear particles accompanying the dynamic shearing/adhesive interactions. Nevertheless, an adhesive film of wear debris agglomerates was formed on the worn surface, leading to conformal sliding contact in the steady state sliding.

4.2 The friction and wear at RT - 200 ^0C

The TiAlN/VN coating retained low friction at the test temperatures up to 100 ^{0}C, and then experienced the first transition to higher friction when the temperature was raised from 100 to 200 ^{0}C. The excellent tribological properties of the TiAlN/VN coatings were attributed to such a particular test environment which favours the tribo-chemical reaction to form the solid lubricant hydroxide tribofilm. When the test temperature was raised to 100 ^{0}C and higher, the absorption of water vapour vanished, leading to significant changes both in the friction behaviour and the wear mechanisms. Similar friction behaviours have been observed in other transition metal nitride coatings, such as TiN [17], VN [19, 33], CrN [12], VTiN [15], and CrAlN/CrN [16].

A reasonable explanation for this phenomenon is that, the adsorption of ambient water vapour as well as other gaseous species on the sliding surfaces would partially break the ionic bonding and thereafter weaken the adhesive attraction. Meanwhile, the adsorbed molecules may also chemically react with the wear debris to form a complex tribofilm of hydro-oxide-nitride. This has been confirmed in the TEM-EELS analysis (Figure 6) for the co-existence of nitrogen and oxygen, whereas the presence of [H-O] bond in the room temperature wear debris was detected by Fourier transform infrared spectroscopy (FTIR) [11, 27]. The hydroxide induced low friction, or solid lubrication, was also found in the fretting wear of a TiN coating under controlled environment humidity, in which the TiN coating showed a linear decrease of friction coefficient from 1.3 to 0.3 with the increased relative humidity from 10% to 90% [34].

The extremely low wear coefficient of the TiAlN/VN coatings, being in a scale of 10^{-17} $m^3N^{-1}m^{-1}$ (Table 2), resulted from the combined low friction during the sliding wear and the super hardness of the coating. Analysis of worn surfaces suggested that the predominant wear mechanism under such test conditions was tribo-oxidation (Figure 6), whereas the worn surface work hardening was marginal (Figure 8) resulting in the prevention of cracking or severe delamination wear. More comprehensive analysis of the wear mechanisms of the TiAlN/VN coatings after RT tribotests has been published elsewhere [9-10].

4.3 The friction and wear at 200 - 400 ^0C

In the test temperatures from 200 to 400 ^{0}C, the friction coefficient was between 0.85 and 0.89. In this temperature period, the vanished water vapour adsorption and the decomposition of the [H-O] bond, seeing literatre [27], resulted in wear debris and tribofilms of hydrogen-free multicomponent oxide. However, the V-O containing oxide tribofilm did not bring about low friction. The experimental finding has updated the previous understanding of the tribological property of TiAlN/VN coatings [8, 9] which concluded that it was the V_2O_5 oxide or the V-O containing multicomponent oxide tribofilm which resulted in the low friction coefficient.

The high friction obtained between 200 and 400 ^{0}C led to the transition from mild oxidation wear to severe mechanical wear, the latter being featured by the increased wear coefficient to the 10^{-16} $m^3N^{-1}m^{-1}$ scale (Table 2),

the occurrence of cracking after 50,000 cycles of sliding, and the catastrophic spalling failure (Figures 9 and 10). According to the theory of tribology, high frictional load may increase the wear loss of material due to the intensified mechanical loading and the increased friction energy dissipation. In the first, the increased friction coefficient results in linear increases of the maximum hoop tensile stress at the trailing edge of the sliding contact and the shear stress on the sliding surface. For the former, the relationship between the friction coefficient (μ) and the maximum tensile stress (σ_{max}) can be expressed as: $\sigma_{max} = 0.0796 \cdot P \cdot (1+10 \cdot \mu)/a^2$, where P, μ and a stand for the applied normal load, the coefficient of friction, and the area of contact respectively [34]. In case of the current study, the σ_{max} values for a fixed applied load of 5N were estimated to be 630 and 900 MPa respectively for the friction coefficients of 0.6 and 0.9, denoting approximately 43% increase of the σ_{max} at the elevated temperatures between 200 and 400 ^{0}C. The increased tensile stress would accelerate the generation of tensile cracks. Similar cracking behaviour was recently report in the high temperature sliding wear of another transition metal nitride coating CrAlYN/CrN [16]. Then concerning the increase tangential loading on the sliding surface, the enhanced worn surface deformation has been indicated by the increased Knoop hardness in the top layer as shown in Figure 8.

In addition, high frictional heating would result in a linear increase of flash temperature in the up-most sliding surface [32, 35, 36]. In the current study, however, the contribution of the increased flash temperature to the wear was in fact relatively marginal as compared to the intensified mechanical wear. Therefore, the predominant influence of the increased friction should be the intensified tensile and shear stresses which caused severe cracking and spalling.

4.4 The friction and wear at above 500 ^{0}C

At 500 ^{0}C and higher test temperatures, it was the oxidation, no longer the sliding wear, which dominated the material loss in the sliding process. This has been evidenced by the massive amount of oxide wear debris agglomerating on the worn surface (Figure 11) and by the occurrence of subsurface oxidation (Figure 12). The steep increase of friction from the temperature of 400 to 500 ^{0}C suggests a transition of the predominant material loss from wear to oxidation. At 500 ^{0}C, a thick tribofilm being involved in the sliding contact resulted in further increase of the friction coefficient to the maximum value. Then between 500 and 700 ^{0}C, the friction behaviour was governed by the shearing resistance of the oxide tribofilm, e.g., lower friction coefficient at 600 ^{0}C when approaching towards the melting point of V_2O_5 oxide (approximately 633^{0}C). Previous cross-sectional TEM found that the V_2O_5 oxide was formed on the top of the oxidised TiAlN/VN coating, in which shearing deformation within the V_2O_5 oxide top layer exhibited a low friction coefficient of 0.46 [27]. Finally, at 700 ^{0}C the test showed the lowest friction coefficient when the sliding contact took place between the alumina ball and the melted V_2O_5. Such low friction due to melted V_2O_5 was firstly observed in TiAlN/VN [16] and subsequently reported in several other vanadium containing nitride coatings [19 - 21]. However, when oxidation had replaced sliding wear as the major surface process, the TiAlN/VN is no longer as a wear resistant material after losing the intrinsic mechanical properties of the nano-structured nitride.

5. Conclusions

In the unlubricated sliding wear tests against an alumina counterface, TiAlN/VN coating showed significant temperature-dependent friction and wear properties in the range of testing temperatures from RT to 700 ^{0}C.

1) At ambient temperatures below 100^{0}C, the coating showed low friction coefficient at $\mu \leq 0.6$ and low wear rate in the scale of 10^{-17} $m^3N^{-1}m^{-1}$.
2) From 100 to 200 ^{0}C, a progressive transition to higher friction coefficient occurred.
3) After that, the coating exhibited high friction of $\mu = 0.9$ at temperatures between 200 and 400 ^{0}C, and simultaneously higher wear rates of (10^{-16} ~ 10^{-15}) $m^3N^{-1}m^{-1}$. The predominant influence of the increased friction has been the intensified tensile and shear stresses which caused severe cracking and spalling.
4) From 500 ^{0}C and so on, accelerated oxidation of the TiAlN/VN became the controlling process. This led first to the massive generation of oxide debris and maximum friction of $\mu = 1.1$ at 500 ^{0}C, and then to fast deterioration of the coating despite the increasingly lower friction coefficient from $\mu = 0.9$ at 600 ^{0}C to $\mu = 0.2 – 0.3$ at 700 ^{0}C.

Acknowledgements

The author would like to thank Dr. Z. Zhou, University of Sheffield, for providing the EELS analysis.

References

[1] W.-D. Münz, L.A. Donohue, P.Eh. Hovsepian, Properties of various large-scale fabricated TiAlN- and CrN-based superlattice coatings grown by combined cathodic arc–unbalanced magnetron sputter deposition, Surf. Coat. Technol. 125 (2000) 269-277.

[2] P. Eh. Hovsepian, Q. Luo, G. Robinson, M. Pittman, M. Howarth, D. Doerwald, R. Tietema, W.M. Sim, M.R. Stalley, TiAlN/VN Superlattice Structured PVD Coatings: A New Alternative in Machining of Al Alloys for Aerospace and Automotive Components, Surf. Coat. Technol. 201 (2006) 265-272.

[3] Q. Luo, P.Eh. Hovsepian, D.B. Lewis, W.-D. Münz, Y.N. Kok, J. Cockrem, M. Bolton, A. Farinotti, Tribological perperties of unbalanced magnetron sputtered nanoscale multilayer coatings TiAlN/VN and TiAlCrYN deposited on plasma nitrided steels, Surf. Coat. Technol. 193 (2005) 39-45.

[4] P.Eh. Hovsepian, D.B. Lewis, W.D. Münz, Recent progress in large scale manufacturing of multilayer / superlattice hard coatings, Surf. Coat. Technol. 133-134 (2000) 166-175.

[5] H. Meidia, A.G. Cullis, C. Schonjahn, W.D. Münz, J.M. Rodenburg, Investigation of intermixing in TiAlN/VN nanoscale multilayer coatings by energy-filtered TEM, Surf. Coat. Technol. 151-152 (2002) 209.

[6] Q. Luo, D.B. Lewis, P.Eh. Hovsepian, W.–D. Münz, Transmission electron microscopy and X-ray diffraction investigation of the microstructure of nano-scale multilayers TiAlN/VN grown by unbalanced magnetron deposition, J. Mater. Res. 19 (2004) 1093-1104.

[7] D.B. Lewis, S. Creasey, Z. Zhou, J.J. Forsyth, A.P. Ehiasarian, P.Eh. Hovsepian, Q. Luo, W.M. Rainforth, W.-D. Münz, The effect of (Ti+Al):V ratio on the structure and oxidation behavior of TiAlN/VN nano-scale multilayer coatings, Surf. Coat. Technol. 177-178 (2004) 252-259.

[8] C.P. Constable, J. Yarwood, P.Eh. Hovsepian, L.A. Donohue, D.B. Lewis, W.-D. Münz, Structural determination of wear debris generated from sliding wear tests on ceramic coatings using Raman microscopy, J. Vac.Sci. Technol. A18 (2000) 1681-1689.

[9] Q. Luo, P. Eh. Hovsepian, Transmission electron microscopy and energy dispersive Xray spectroscopy on the worn surface of nano-structured TiAlN/VN multilayer coating, Thin Solid Films, 497 (2006) 203-209.

[10] Q. Luo, Z. Zhou, W.M. Rainforth, P. Eh. Hovsepian, TEM-EELS study of low-friction superlattice TiAlN/VN coating: The wear mechanisms, Tribo. Lett. 24 (2006) 171-178.
[11] Z. Zhou, W.M. Rainforth, C.C. Tan, P. Zeng, J.J. Ojeda, M.E. Romero-Gonzalez, P.Eh. Hovsepian, The role of the tribofilm and roll-like debris in the wear of nanoscale nitride PVD coatings, Wear 263 (2007) 1328-1334.
[12] T. Polcar, L. Cvrcek, P. Siroky, R. Novak, Tribological characteristics of CrCN coatings at elevated temperature, Vacuum 80 (2005) 113-116.
[13] J.G. Han, J.S. Yoon, H.J. Kim, K. Song, High temperature wear resistance of (TiAl)N films synthesized by cathodic arc plasma deposition, Surf. Coat. Technol. 86-87 (1996) 82-87.
[14] G. Lopez, M.H. Staia, High temperature tribological characterization of zirconium nitride coatings, Surf. Coat. Technol. 200 (2005) 2092-2099.
[15] J.H. Ouyang, T. Murakami, S. Sasaki, High temperature tribological properties of a cathodic arc ion-plated (V,Ti)N coating, Wear 263 (2007) 1347-1353.
[16] J.C.Walker, I.M. Ross, C. Reinhard,W.M. Rainforth, P.Eh. Hovsepian, High temperature tribological performance of CrAlYN/CrN nanoscale multilayer coatings deposited on γ-TiAl, Wear 267 (2009) 965-975.
[17] E. Badisch, G.A. Fontalvo, M. Stoiber, C. Mitterer, Tribological behavior of PACVD TiN coatings in the temperature range up to 500 0C, Surf. Coat. Technol. 163-164 (2003) 585-590.
[18] P.H. Mayrhofer, P.Eh. Hovsepian, C. Mitterer, W.-D. Münz, Calorimetric evidence for frictional self-adaptation of TiAlN/VN superlattice coatings, Surf. Coat. Technol. 177- 178 (2004) 341-347.
[19] N. Fateh, G.A. Fontalvo, G. Gassner, C. Mitterer, The beneficial effect of high-temperature oxidation on the tribological behaviour of V and VN coatings, Tribo. Lett. 28 (2007) 1-7.
[20] R. Franza, J. Neidhardt, B. Sartory, R. Kaindl, R. Tessadri, P. Polcik, V.H. Derflinger, C. Mitterer, High-temperature low-friction properties of vanadium-alloyed AlCrN coatings, Tribo. Lett. 23 (2006) 101-107.
[21] Z. Zhou, W.M. Rainforth, Q. Luo, P.Eh. Hovsepian, J.J. Ojeda, M.E. Romero- Gonzalez, Wear and friction of TiAlN/VN coatings against Al2O3 in air at room and elevated temperatures, Acta Mater. 58 (2010) 2912-2925.
[22] W.D. Münz, I.J. Smith, D.B. Lewis, S. Creasey, Droplet formation on steel substrates during cathodic steered arc meytal ion etching, Vacuum 48 (1997) 473-481.
[23] F. Hofer, P. Warbichler, A. Scott, R. Brydson, I. Galesic, B. Kolbesen, J. Microscopy 204 (2001) 166-171.
[24] C. Mitterbauer, C. Hebert, G. Kothleitner, F. Hofer, P. Schattschneider and H.W. Zandbergen, Solid State Commun. 130 (2004) 209-213.
[25] M. MacKenzie, A.J. Craven and C.L. Collins, Scripta Mater 54 (2006) 1-5.
[26] Q. Luo, Origin of friction in running-in sliding wear of nitride coatings, Tribo. Lett. 37 (2010) 529-539.
[27] Q. Luo, Z. Zhou, W.M. Rainforth, M. Bolton, Effect of tribofilm formation on the dry sliding friction and werar properties of magnetron sputtered TiAlCrYN coatings, Tribo. Lett 34 (2009) 113-124.
[28] Z. Zhou, W.M. Rainforth, C. Rodenburg, N.C. Hyatt, D.B. Lewis, P.E. Hovsepian, Oxidation behaviour and mechanisms of TiAlN/VN coatings, Metall. Mater. Trans 38A (2007) 2464-2478.
[29] Q. Luo, W.M. Rainforth, W.-D. Münz, TEM study of the wear of TiAlN/CrN superlattice coatings, Script. Mater. 45 (2001) 399-404.
[30] Q. Luo, W.M. Rainforth, W.-D. Münz, Wear mechanisms of monolithic and multicomponent nitride coatings grown by combined arc etching and unbalanced magnetron sputtering, Surface and Coatings Technology, 146 –147 (2001) 430 –435.
[31] S.T. Oktay, N.P. Suh, Wear debris formation and agglomeration, Trans. ASME –J. Tribo. 114 (1992) 379-393.
[32] T.F. Quinn, Review of oxidation wear, Part I, Tribo. Int. 16 (1983) 257-271.
[33] M.Z. Huq, J.P. Celis, Expressing wear rate in sliding contacts based on dissipated energy, Wear 252 (2002) 375-383.
[34] H.R. Pasaribu, J.W. Sloetjes, D.J. Schipper, The transition of mild to severe wear of ceramics, Wear 256 (2004) 585-591.
[35] M. Kalin, J. Vizintin, Comparison of different theoretical models for flash temperature calculation under fretting conditions, Tribo. Int. 34 (2001) 831-839.
[36] E. Vancoille, B. Blanpain, X. Ye, J.P. Celis, J.R. Roos, Tribo-oxidation of a TiN coating sliding against corundum, J. Mater. Res. 9 (1994) 992-999.